Synthesis and Characterization of Upper and Lower Rim Functionalized [6]Cavitands

Christoph Naumann, Brian O. Patrick, and John Sherman*[a]

Abstract: A [6]cavitand has been selectively derivatized on both the lower and upper rims. On the lower rim, two out of six potential sites were oxidized to produce a 1,4 substituted [6]cavitand bisketone, which was converted to a corresponding diol as well as a bisacetate [6]cavitand. The crystal structures of the bisketone and the diol were solved. On the upper rim, all six $ArCH_3$ groups were selectively brominated to $ArCH_2Br$ groups to produce the hexabromomethyl [6]cavitand, which was converted to the corresponding hexabenzylthiol and hexabenzylthioacetate [6]cavitands. The conformational properties of all compounds are discussed.

Keywords: cavitands · interconversion · NMR spectroscopy · supramolecular chemistry

Introduction

[4]Cavitands have been known for 20 years and have found use in numerous supramolecular applications such as in recognition of neutral guests and as building blocks to create carceplexes.[1–3] Recently we reported the synthesis and characterization of the first [*n*]cavitands, where $n = 5-7$.[4] All possess benzylic methyl groups on the upper rims and $ArCH_2Ar$ groups on the lower rims (Figure 1). The lower rims

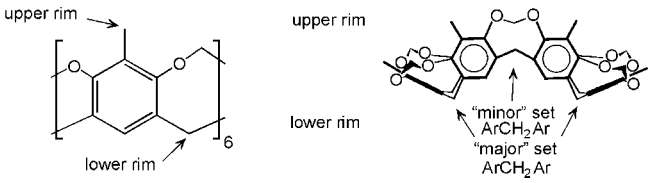

Figure 1. Upper and lower rims, "major" and "minor" sets of [6]cavitand **1**.

are unusual; common [4]cavitands possess ArCH(R)Ar groups.[1–3] The R groups typically enhance the solubility of [4]cavitands and [4]cavitand-based derivatives such as carceplexes.[3] In addition, methyl groups on the upper rim can be selectively brominated when R groups are present in the lower rim, since the reactivity of the methine is low. However, in the case of the footless [*n*]cavitands, the $ArCH_2Ar$ may be vulnerable to attack as well. We recently reported that [5]cavitands can be selectively brominated on the upper rim.[5] The [6]cavitands are structurally quite different from the [4]- and [5]cavitands, and thus offer new possibilities for cavitand supramolecular chemistry. But one might be concerned about the potential limitations for derivatization of [6]cavitands for the reasons given. We report the successful derivatization at the upper rim of [6]cavitand **1** despite the potentially vulnerable lower rim. We also describe the selective derivatization of [6]cavitand **1** at the lower rim. The structure and dynamics of the new compounds are discussed in detail. This diversification of the [*n*]cavitands will hopefully enhance their utility to supramolecular chemists.

[a] Prof. J. Sherman, C. Naumann, B. O. Patrick
Department of Chemistry
University of British Columbia
2036 Main Mall, Vancouver, BC, V6T 1Z1 (Canada)
Fax: (+1) 604-822-2305
E-mail: sherman@chem.ubc.ca

Results and Discussion

Derivatization of the lower rim

To set the stage for characterization of compounds **2**–**9**, the symmetry and exchange pattern for **1** is summarized here.[4] Whereas [4]- and [5]cavitands are rigid, bowl-shaped molecules of C_{4v} and C_{5v} symmetry, respectively, [6]cavitands, as well as [7]cavitands, are pinched and conformationally mobile. Prototypical [6]cavitand **1** possesses "major" and "minor" sets of resonances in 2:1 ratios (Figure 1).[4] For example, the twelve $ArCH_2Ar$ protons appear at four different resonances: H_5, H_9 (4H each), and H_8, H_{10} (2H each). 1D NOESY (EXSY) experiments[6] demonstrated that exchange occurs between H_8 and H_9 (2H: 2H), and H_5 and H_{10} (2H: 2H), as illustrated in Figure 2.[4] The remaining four protons of the "major" set (2H each of H_5 and H_9) interconvert into themselves, an NMR silent process (Figure 2b).

 © 2002 WILEY-VCH Verlag GmbH & Co. KGaA, Weinheim 0947-6539/02/0816-3717 $ 20.00+.50/0

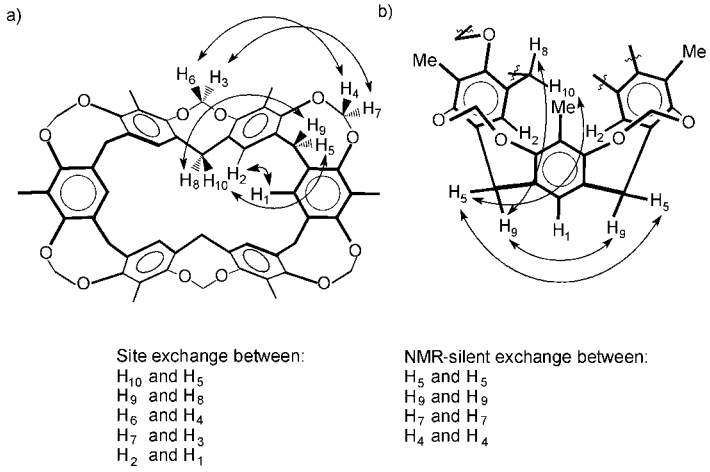

Figure 2. Illustration of exchange in [6]cavitand **1**: a) as seen from the lower rim. b) Side view: only half of the molecule is shown for clarity; the OCH_2O protons are not labeled.

[6]Cavitands **2**–**4** were prepared as follows (Scheme 1): treatment of [6]cavitand **1** with $KMnO_4$ led to an oxidation product (39%) that we assign as bisketone **2**.[7] Reduction of bisketone **2** with $LiAlH_4$ gave diol **3** (32%), followed by acetylation to bisacetate **4** (73%).

Bisketone **2** was characterized as follows: The mass spectrometry and ^{13}C NMR results suggest that oxidation of **1** gave a conjugated bisketone (δ_{CO} = 186 ppm). Thus, the oxidation is selective at the lower rim for reasons that remain unclear, and there is high selectivity for oxidation of only two of the six $ArCH_2Ar$ moieties, presumably due to the unfavorable conformation (with respect to orbital overlap of $ArCH\cdot$/$ArCH^+$ with the arenes) at the remaining sites. The ^1H NMR spectrum indicates that the two carbonyls are in 1,4 positions: in $CDCl_3$, at $-10\,^\circ C$ there are three resonances for the six ArH protons at 2H each, and two of the three ArH resonances interconvert ($H_{2'}$ and $H_{2''}$).[8, 9] Similarly, diol **3** shows three *para* ArH signals at 2H each, two of which interconvert, (H_1 and $H_{2''}$).[9] Bisacetate **4** possesses a very similar ^1H NMR spectrum to diol **3**.

Compounds **2**–**4** can exist in two basic 1,4 conformations: **I** and **II**, which differ in the locations of the lower R groups (R = O, OH, OAc, respectively) as illustrated in Figure 3. In conformation **I**, the R groups are situated at the corners of the rectangularly shaped [6]cavitand, whereas in conformation **II** the R groups are situated in the middle of the long sides of the rectangle. Conformation **I** is consistent with solution data for diol **3** and bisacetate **4** (vide infra), and the crystal structure of diol **3** (Figure 4). Neither conformation **I** nor conformation **II** are consistent with the ^1H NMR data for bisketone **2** (vide infra). The crystal structure of **2** (Figure 5) shows a lower symmetry version of **II** (chiral conformation **IIa**, Figure 3), which is consistent with the solution data as well (vide infra).

Conformers **I** and **IIa** should yield telling chemical shift differences for the potentially exchanging resonances x (x', x''), and y (Figure 3; see also Figure 6 for the OCH_2O and $ArCH_2Ar$ parts of the ^1H NMR spectra for compounds **1**–**3**). The corresponding $\Delta\delta$ values are shown in Table 1. With the exception of the ArH protons, the $\Delta\delta$ values for **3** and **4** range

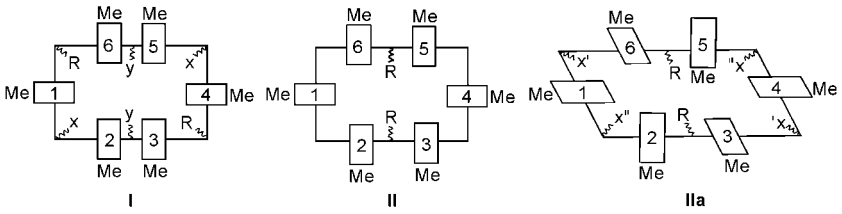

Figure 3. Schematic drawings of the possible conformations of compounds **2**–**4** (R = O, OH, OAc, respectively). The numbers represent the six arenes. The letters x (x', x''), and y stand for $ArCH_2Ar$ or OCH_2O resonances situated in similar (x', x'') or different (x, y) chemical environments.

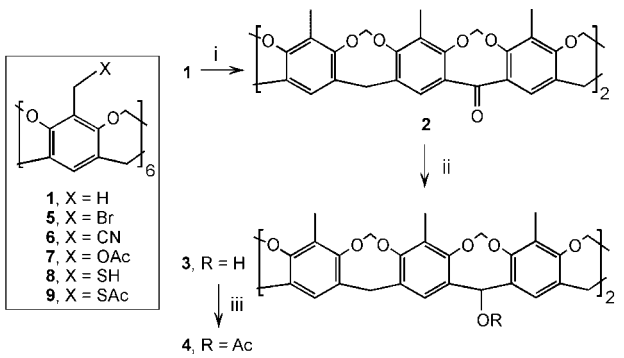

Scheme 1. Synthesis of lower rim derivatives of [6]cavitand **1**: i) $KMnO_4$, 60 °C, DMA, 39%; ii) $LiAlH_4$, THF; H^+/H_2O, 32%; iii) acetic anhydride, pyridine, 73%.

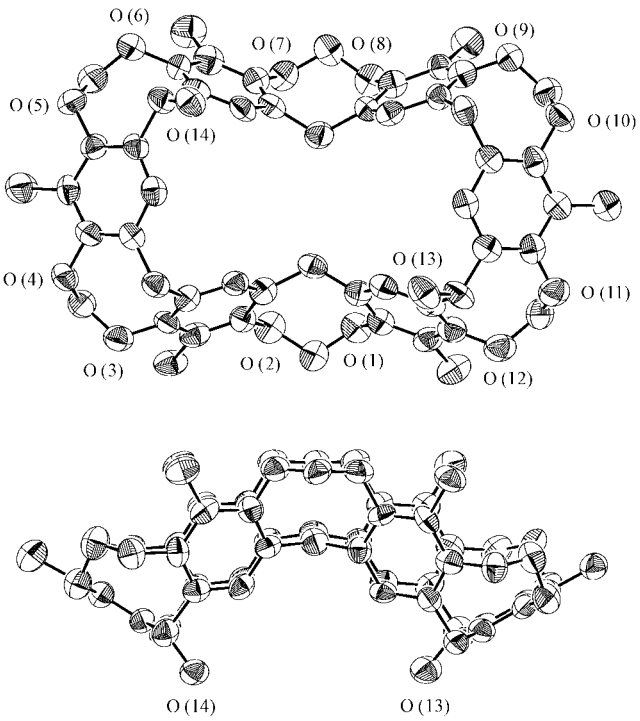

Figure 4. Two views (ORTEP plot at 50% probability) of the X-ray crystal structure of the diol **3**. The unit cell also contained six acetone molecules and another, marginally different diol **3**. Hydrogen atoms are omitted for clarity. The diol oxygen atoms are O(13) and O(14).

© 2002 WILEY-VCH Verlag GmbH & Co. KGaA, Weinheim
0947-6539/02/0816-3718 $ 20.00+.50/0 *Chem. Eur. J.* **2002**, *8*, No. 16

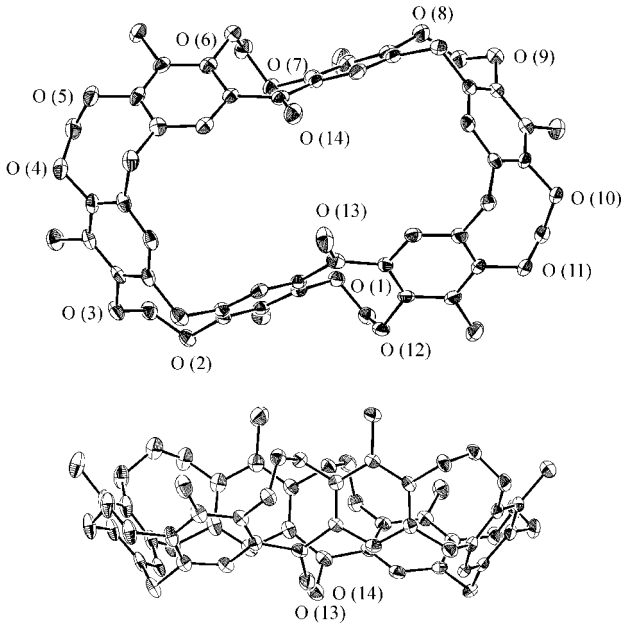

Figure 5. Two views (ORTEP plot at 50 % probability) of the X-ray crystal structure of the bisketone **2**. The unit cell also contained six [D_6]DMSO molecules and another, marginally different bisketone **2**. Hydrogen atoms are omitted for clarity. The ketone oxygen atoms are O(13) and O(14).

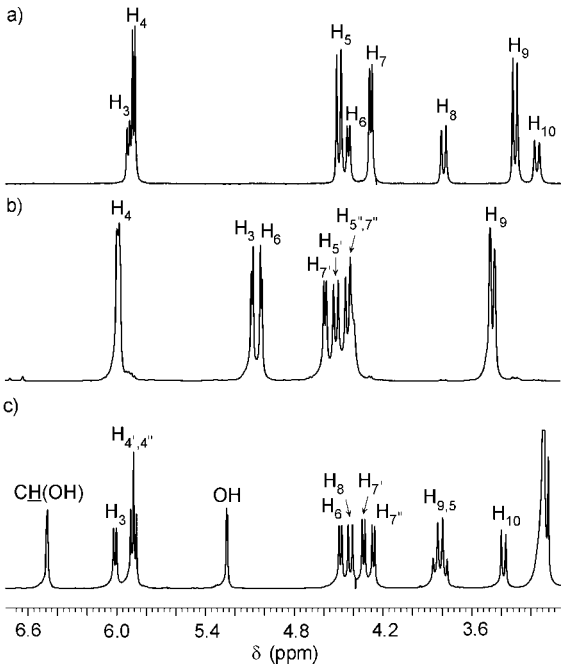

Figure 6. Parts of the ^{1}H NMR spectra of a) [6]cavitand **1** in $CDCl_3$, b) bisketone **2** in $CDCl_3$, c) diol **3** in [D_6]acetone. The aromatic protons and the methyl protons are not shown. All spectra were recorded at $-10\,^\circ$C. See Figure 2 for labels of [6]cavitand **1**. Labels for **2** are given in Figure 7. Labels for **3** are given in Figure 9.

from 0.4 – 1.7 ppm. Such large ranges arise from the markedly different shielding effects in the "corner" and "center" positions in conformation **I** ("major" and "minor" sets in Figure 1; positions *x* and *y* in Figure 3). Similar $\Delta\delta$ ranges were observed for the prototype [6]cavitand **1** (Table 1 and Figure 2).[4] In contrast, the $\Delta\delta$ values for bisketone **2** are much smaller, which means such pairs of protons must be in

Table 1. ^{1}H NMR ($-10\,^\circ$C, 400 MHz) chemical shift differences [ppm] between exchanging resonances for **1**–**4**. Labeling for compounds **1**–**4** refers to Figure 2, 7, and 9, respectively.

		ArH	OCH_2O		$ArCH_2Ar$	
1[a]	exchanging sets	H_1,H_2	H_3,H_7	H_4,H_6	H_5,H_{10}	H_8,H_9
	$\Delta\delta$ [ppm]	0.05	1.64	1.45	1.33	0.48
2[a]	exchanging sets	$H_{2'}$,$H_{2''}$	$H_{7'}$,$H_{7''}$		$H_{5'}$,$H_{5''}$	
	$\Delta\delta$ [ppm]	0.44	0.17		0.09	
3[b]	exchanging sets	H_1,$H_{2''}$	H_3,$H_{7'}$	$H_{4'}$,H_6	H_5,H_{10}	H_8,H_9
	$\Delta\delta$ [ppm]	0.21	1.68	1.40	0.42	0.61
4[b]	exchanging sets	H_1,$H_{2''}$	H_3,$H_{7'}$	$H_{4'}$,H_6	H_5,H_{10}	H_8,H_9
	$\Delta\delta$ [ppm]	0.11	1.66	1.38	0.37	0.65

[a] In $CDCl_3$. [b] In [D_6]acetone.

very similar environments, indicating that bisketone **2** exists in solution in conformation **IIa**.

Conformation of bisketone 2: Computer modeling[10] supports the conclusion that bisketone **2** exists in conformation **IIa** (Figure 3). The steric energy difference between conformers **IIa** and **I** was calculated to be 24 kcal mol^{-1}. Conformer **IIa** is more stable than conformer **I** likely because of increased conjugation and reduced angle strain for the carbonyls. We conducted a detailed analysis of the exchange pattern for bisketone **2** by 1D NOESY (EXSY) experiments[6] (in $CDCl_3$, at $-10\,^\circ$C, at 400 MHz) to support the conformational conclusions and to explore the dynamic properties of **2**. In conformation **IIa**, a diagonal pair of the four arenes (arenes 3 and 6, Figure 3) next to the carbonyl ligands is twisted towards each other to almost parallel planes, which results in the carbonyls being in rather "feet"-like positions (Figure 5). That geometry reduces the symmetry, and as a result, the H_5 and H_7 protons each split into two interconverting resonances ($H_{5'}$, $H_{5''}$ and $H_{7'}$, $H_{7''}$, see Figure 6). Irradiation of the $H_{7'}$ resonance yields exchange at $H_{7''}$, and irradiation at $H_{5'}$ yields exchange at $H_{5''}$ (Figure 7). $H_{5'}$ and $H_{5''}$ are both correlated by

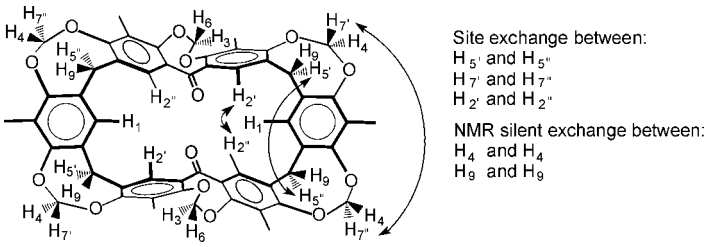

Figure 7. Illustration of exchange in bisketone [6]cavitand **2** as seen from the lower rim.

COSY to H_9, but not to each other. The H_9 protons should be split in $H_{9'}$ and $H_{9''}$, but the resonances likely coincide. Similarly, $H_{7'}$ and $H_{7''}$ are both correlated by COSY to H_4, but not to each other; H_4' and $H_{4''}$ coincide. In conformation **I**, the H_9 and H_4 protons would both be situated in two very different positions (*x* and *y* in Figure 3), and coinciding resonances are highly unlikely. A schematic drawing of the interconversion of conformational enantiomers of bisketone **2** is shown in Figure 8. The activation barrier for this inter-

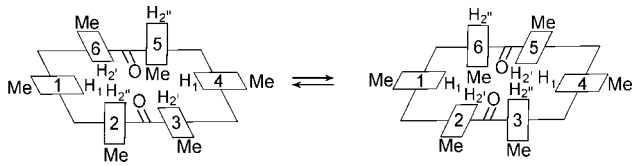

Figure 8. Interconversion of conformational enantiomers of bisketone **2**. The numbers 1 to 6 represent the six arenes. Interconversion between the aromatic *para* protons $H_{2'}$ and $H_{2''}$ is shown as an example; the same is true for the other exchanging resonances in **2** ($H_{5'}/H_{5''}$ and $H_{7'}/H_{7''}$).

conversion was determined by 1D NOESY (EXSY) experiments[6] (at $-10\,^{\circ}C$, both in $CDCl_3$ and [D_6]acetone), and found to be 14.8 kcal mol^{-1} (Table 2).

Table 2. Summary of activation barriers for interconversion of [6]cavitands **1**–**4** obtained by 1D NOESY (EXSY) experiments at different temperatures at 400 MHz. The rate constants were obtained by initial rate approximation;[6] errors for rate constants are ±20%.

Compound	T [°C]	Solvent	Irradiated proton	k [s^{-1}]	$\Delta G^{\ddagger}_{263}$ [kcal mol^{-1}][a]
1	−10	$CDCl_3$	H_8	2.2	14.9
2	−10	$CDCl_3$	$H_{2''}$	3.0	14.8
	−10	[D_6]acetone	$H_{2''}$	2.9	14.8
3	−10	[D_6]acetone	H_1	0.14	16.3
	5	[D_6]acetone	H_1	1.0	16.2
	26	[D_6]acetone	H_1	6.5	16.4
	26	MeOD	H_1	5.4	16.5
4	5	[D_6]acetone	H_{10}	3.8	15.5
5	−10	$CDCl_3$	H_3	1.7	15.0
8	−10	$CDCl_3$	H_8	0.30	16.0
	26	$CDCl_3$	H_9	10.0[b]	16.1
9	26	$CDCl_3$	H_{12}	6.6	16.4

[a] ± 0.1 kcal mol^{-1}. [b] Corrected for NMR-silent protons.

Characterization of the diol and bisacetate products 3 and 4: Computer modeling[10] suggests that diol **3** and bisacetate **4** exist in conformation **I**, which is in agreement with the crystal structure. The difference in steric energy between conformers **I** and **IIa** was calculated to be 10 kcal mol^{-1} for **3** and 11 kcal mol^{-1} for **4**. The "axial" diastereotopic position of the hydroxy groups in diol **3** (Figure 9b) can be seen in the crystal structure but was independently derived from the exchange and NOE data.[11]

The chemical shift, exchange, and NOE pattern for bisacetate **4** is identical to that observed for diol **3**, which implies that the compounds exist in the same conformation. For both diol **3** and bisacetate **4**, $H_{4''}$ and $H_{7''}$ do not manifest any exchange, whereas the other acetal resonances (H_3, $H_{4'}$, H_6, $H_{7'}$) exchange with each other. The interconversion of diol **3** and bisacetate **4** is summarized in Figure 10. The activation barriers for interconversion of identical conformers was determined by 1D NOESY (EXSY) experiments[6] for **3** and **4** (at 5 °C, in [D_6]acetone), and found to be 16.2 and 15.5 kcal mol^{-1}, respectively (see Table 2). The free hydroxyl groups of **3** lead to a fourfold reduction in rate compared to that for **4**.

Derivatization on the upper rim

[6]Cavitand **1** was derivatized on its upper rim by radical bromination at the benzylic methyl groups to give **5** (24%)

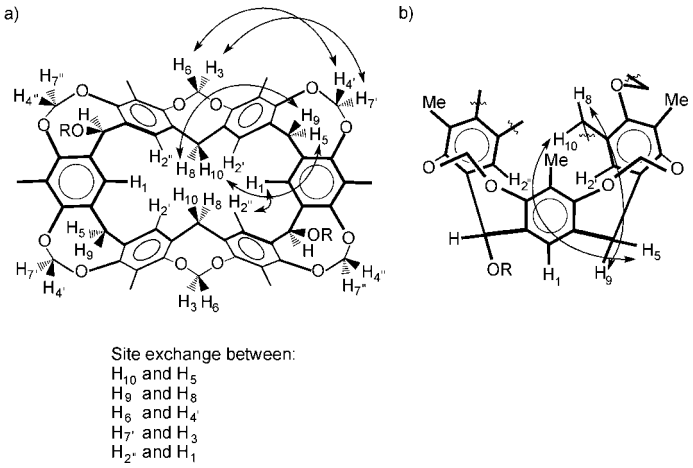

Figure 9. Illustration of exchange in diol **3** (R = H) and bisacetate **4** (R = Ac); conformation **I** is shown: a) as seen from the lower rim. b) side view: only half of the molecule is shown for clarity; the OCH_2O protons are not labeled; the OR groups are in "axial" positions.

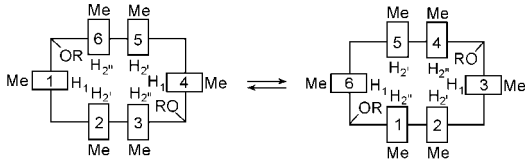

Figure 10. Interconversion for diol **3** (R = H) and bisacetate **4** (R = Ac). The numbers 1 to 6 represent the six arenes. Conformation **I** is shown (Figure 3).

(Scheme 1). Yields were expected and found to be lower than those reported for cavitands having the lower rim position blocked from radical attack by the presence of "feet". Indeed, considerable selectivity is required to produce **5**, where bromination must occur at six $ArCH_3$ groups, with no bromination at six Ar_2CH_2 groups.[12]

Characterization of the bromination product 5: To acertain that benzyl bromide **5** contains all bromines on the upper rim, the ^{1}H NMR spectrum of **5** was obtained at −9 °C in $CDCl_3$ at 400 MHz (Figure 11). The 2:1 symmetry of [6]cavitand **1** is

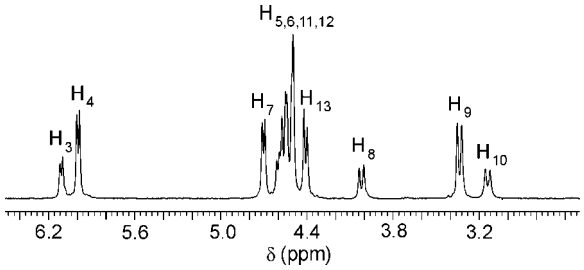

Figure 11. Parts of the ^{1}H NMR spectra of **5**. Labels are given in Figure 12 and are based on the general labeling for [6]cavitand **1** in Figure 2.

retained. For instance, the $ArCH_2Ar$ protons appear as four doublets, two of which correspond to 4H each, and two to 2H each, the same "major" and "minor" set situation as in [6]cavitand **1** (see Figure 12a for labeling). The two benzylic methyl resonances of [6]cavitand **1** (12H and 6H) are not present in **5**, but are replaced by two sets of doublets of 4H

© 2002 WILEY-VCH Verlag GmbH & Co. KGaA, Weinheim
0947-6539/02/0816-3720 $ 20.00+.50/0 *Chem. Eur. J.* **2002**, *8*, No. 16

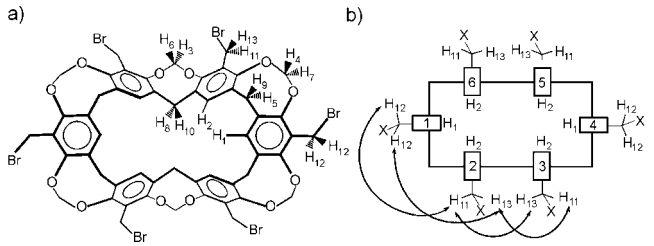

Figure 12. a) Labeling of benzyl bromide **5** based on COSY and 1D NOESY experiments; b) Schematic drawing of exchange of $ArCH_2X$ protons in **5** (X = Br) and **9** (X = SAc).

each and one singlet of 4H: the benzyl bromide protons of the former "major" set of the benzyl methyls are diastereotopic and split in two doublets that show a geminal correlation by COSY experiments, whereas the "minor" set $ArCH_2Br$ protons (H_{12}) are equivalent (enantiotopic). Irradiation of the only accessible $ArCH_2Br$ resonance (the doublet for H_{13}, see Figure 11) yields equal responses at H_{11} and H_{12}. The exchange seen between diastereotopic protons demonstrates that **5** interconverts much the same as does **1** (see Figure 2 and Figure 12b). The activation barriers for [6]cavitands **5** and **1** are almost the same (Table 2).

Further derivatizations of benzyl bromide 5: Benzyl bromide [6]cavitand **5** was converted to benzylthiol **8** in 56% yield using standard conditions.[13] No clear signal was observed in the MALDI-MS of **8**. To confirm the structure, **8** was acetylated, resulting in benzylthioacetate **9**. The MALDI spectrum of **9** shows peaks at *m*/*z* 1356 and *m*/*z* 1372 for the sodium and potassium adducts. Benzylthioacetate **9** shows the same exchange pattern as benzyl bromide **5**. For instance, the two positions for the singlet $ArCH_2SAc$ resonance (H_{12}) exchange into either of the two doublet $ArCH_2SAc$ resonances (H_{11} and H_{13}). The activation barriers for benzylthiol **8** (measured exchange between H_8 and H_9) and benzylthio acetate **9** are somewhat larger than those for benzyl bromide **5** and [6]cavitand **1**, as measured by 1D NOESY.

All rate constants for the interconversion processes in **2**–**9** are summarized in Table 2.[6] The similar energy barriers for [6]cavitands **3**–**9** indicate that the interconversion of identical conformers (**I**) is not highly sensitive to derivatization at the upper ($ArCH_3$) or lower ($ArCH_2Ar$) rims.

Conclusion

[6]Cavitand **1** was selectively derivatized on the upper and lower rim and thus, the door is open to a large variety of potential new supramolecular chemistry. Especially interesting is the conformational control, for example, on going from bisketone **2** to diol **3**. Based on solution and solid-state data we showed that diol **3** (conformation **I**) is very similar in shape (the two sets of three arenes form two cavities that are "bent" with respect to each other) to the parent molecule [6]cavitand **1**.[4] In contrast, bisketone **2** (conformation **IIa**) is much less bent, and may offer a conformational alternative for upper and lower rim derivatizations of [6]cavitands. For example, upper rim derivatives in conformation **IIa** could lead to capsular dimers, while derivatives in conformation **I** may form trimers or higher oligomers. Conformation **IIa** versions of benzylthiol **8** might be good candidates for template assembled synthetic proteins (TASP).[14, 15] Alternatively, the two hydroxy groups of diol **3** could be used to form water-soluble [6]cavitands, or the lower rim could be used to form well-defined linkages: The problem with common [4]cavitands substituted in the lower rim (having conformationally mobile "feet" such as the hydroxypropyl group) is the reduced influence of the cavitand to preorganize the self-assembly of the lower rim functional groups.[16, 17] The two hydroxy groups on **3** are conformationally immobile, and the formation of intramolecular complexes should be easily avoided by judicious choice of linkers. It will be interesting to see the effect of conformational interconversion on future designs of higher complexity.

Experimental Section

General: All chemicals were reagent grade and were not specially dried before use, except THF, which was dried over Na and freshly distilled before use. Matrix-assisted laser desorption ionization (MALDI) mass spectra were recorded on a VG Tofspec in reflectron mode; the matrix was *p*-nitroaniline. Liquid secondary ionization mass spectra (LSIMS) were submitted to the mass spectrometry service laboratory at the chemistry department and were run on a Kratos Concept IIH32. ^{1}H NMR spectra were recorded on a Bruker Avance 400 MHz or a Bruker AVA 500 MHz spectrometer using the residual ^{1}H of the deuterated solvent as a reference. Column chromatography was performed using silicycle 230–400 mesh silica gel. Silica gel glass-backed analytical plates (0.2 mm, Aldrich) were used for thin layer chromatography, with UV detection.

Analysis of 1D NOESY spectra: One-dimensional 1D NOESY (EXSY) NMR spectra were recorded on a Bruker AVA 400 MHz spectrometer at different temperatures. The pulse sequence used was selnogp.2 (avance-version-00/02/07), a 1D NOESY that uses selective refocussing with a shaped pulse. Dipolar coupling may be due to NOE or chemical exchange.[6]

Synthesis of bisketone [6]cavitand 2: $KMnO_4$ (4.0 g, 25.3 mmol) was added to a mixture of [6]cavitand **1** (4.0 g, 4.5 mmol) in DMA (300 mL). The clear solution was stirred overnight at ambient temperature. The reaction mixture was filtered, and the brown precipitate was rinsed thoroughly with DMA. The combined DMA fractions were evaporated to dryness under reduced pressure. The dark residue was taken up in acetone, and precipitated starting material was removed by filtration. The filtrate was evaporated to dryness, and the resulting crude product was dissolved in $CHCl_3$ and purified by column chromatography using the same solvent as eluent. The remaining starting material eluted first, after that **2** was obtained as a white powder after removal of the chloroform (1.6 g, 39% yield). Also, a significant amount of starting material was obtained (1.5 g, 38% yield). An alternative synthesis is to stir the **1**/$KMnO_4$ mixture for 2 h at 60 °C. Similar yields were obtained. ^{1}H NMR (400 MHz, $CDCl_3$, −10 °C): δ = 8.09 (s, 2H; ArH; $H_{2'}$), 7.65 (s, 2H; ArH; $H_{2''}$), 7.19 (s, 2H; ArH; H_1), 5.99 (m, 4H; OCH_2O; H_4), 5.08 (d, ^2J(H,H) = 4.7 Hz, 2H; OCH_2O; H_3), 5.02 (d, ^2J(H,H) = 4.7 Hz, 2H; OCH_2O; H_6), 4.59 (d, ^2J(H,H) = 6.8 Hz, 2H; OCH_2O; $H_{7'}$), 4.52 (d, ^2J(H,H) = 12.4 Hz, 2H; $ArCH_2Ar$; $H_{5'}$), 4.43 (d, ^2J(H,H) = 12.4 Hz, 2H; $ArCH_2Ar$; $H_{5''}$), 4.42 (s (br), 2H; OCH_2O; $H_{7''}$), 3.46 (d, ^2J(H,H) = 12.3 Hz, 4H; $ArCH_2Ar$; H_9), 2.11 (s, 6H; $ArCH_3$), 2.05 (s, 6H; $ArCH_3$), 1.99 (s, 6H; $ArCH_3$); HRMS (+LSIMS, 3-NBA): 917.28136, Dev: 0.47 ppm, 54 (^{12}C), 45 (^{1}H), 14 (^{16}O).

Synthesis of diol [6]cavitand 3: Bisketone **2** (0.50 g, 0.54 mmol) was dissolved in freshly distilled THF (50 mL), and excess $LiAlH_4$ (0.1 g, 2.6 mmol) was added carefully. The suspension was stirred for two hours at ambient temperature. The reaction was quenched by addition of H_2O, and the THF was removed under reduced pressure. The reaction mixture was acidified (dilute HCl), and extracted with $CHCl_3$ and in a second step with ethyl acetate. The organic phases were combined, dried, and the solvents

were removed under reduced pressure. The remaining solid was purified by column chromatography using an eluent mixture of $CH_2Cl_2/CH_3OH =$ 98.5:1.5 (v/v). The first eluting product was not fully characterized and is presumed to be an epimer of **3** (OH in axial and equatorial positions) according to its mass spectrum and the fact that it shows six resonances for the *para* ArH protons (0.31 g, 62% yield), followed by **3** (0.16 g, 32% yield). Diol **3** can also be obtained directly from [6]cavitand **1** by treating the crude oxidation-step mixture with $LiAlH_4$. The epimeric product of **3** can be oxidized to bisketone **2** ($KMnO_4$, DMA). ^{1}H NMR (400 MHz, [D$_6$]acetone, $-10\,^\circ$C): $\delta = 7.90$ (s, 2H; ArH; H$_1$), 7.70 (s, 2H; ArH; H$_{2'}$), 7.69 (s, 2H; ArH; H$_{2''}$), 6.47 (d, ^2J(H,H) = 3.2 Hz, 2H; ArCH(OH)Ar), 6.01 (d, ^2J(H,H) = 7.60 Hz, 2H; OCH_2O; H$_3$), 5.89 (dd, 4H; OCH_2O; H$_{4'}$, H$_{4''}$), 5.25 (d, ^2J(H,H) = 3.3 Hz, 2H; OH), 4.49 (d, ^2J(H,H) = 7.5 Hz, 2H; OCH_2O; H$_6$), 4.42 (d, ^2J(H,H) = 11.6 Hz, 2H; $ArCH_2Ar$; H$_8$), 4.33 (d, ^2J(H,H) = 7.4 Hz, 2H; OCH_2O; H$_{7'}$), 4.26 (d, ^2J(H,H) = 7.1 Hz, 2H; OCH_2O; H$_{7''}$), 3.81 (dd, 4H; $ArCH_2Ar$; H$_9$, H$_5$), 3.39 (d, ^2J(H,H) = 11.9 Hz, 2H; $ArCH_2Ar$; H$_{10}$), 2.04 (s, 12H; $ArCH_3$), 2.03 (s, 6H; $ArCH_3$); MALDI-MS: 943 [$M\cdot Na^+$], calcd: 943.3; 959 [$M\cdot K^+$], calcd: 959.3.
HRMS (+LSIMS, 3-NBA): 920.30398, Dev: -0.47 ppm, 54 (^{12}C), 48 (^{1}H), 14 (^{16}O).

Synthesis of bisacetate [6]cavitand 4: A sample of **3** (100 mg, 0.11 mmol) was dissolved in pyridine/acetic anhydride (1:1 (v:v; 20 mL)). The reaction mixture was stirred at ambient temperature overnight. The liquids were removed under reduced pressure, and the residue was dissolved in $CHCl_3$, and purified by column chromatography using chloroform as the eluent to yield **4** as a white powder (80 mg, 73% yield). ^{1}H NMR (400 MHz, [D$_6$]acetone, 5 °C): $\delta = 7.72$ (s, 2H; ArH; H$_{2'}$), 7.67 (s, 2H; ArH; H$_1$), 7.56 (s, 2H; ArH; H$_{2''}$), 7.41 (s, 2H; ArCH(OAc)Ar), 6.02 (d(br), 2H; OCH_2O; H$_3$), 5.94 (d, ^2J(H,H) = 7.4 Hz, 2H; OCH_2O; H$_{4''}$), 5.91 (d, ^2J(H,H) = 7.4 Hz), 2H; OCH_2O; H$_{4'}$), 4.53 (d(br), 2H; OCH_2O; H$_6$), 4.45 (d, ^2J(H,H) = 11.9 Hz, 2H; $ArCH_2Ar$; H$_8$), 4.36 (d, 2H; OCH_2O; H$_{7'}$), 4.33 (d, ^2J(H,H) = 7.3 Hz, 2H; OCH_2O; H$_{7''}$), 3.80 (dd, ^2J(H,H) = 12.5 Hz, 12.7 Hz, 4H; $ArCH_2Ar$; H$_5$, H$_9$), 3.43 (d, ^2J(H,H) = 12.5 Hz, 2H; $ArCH_2$-Ar; H$_{10}$), 2.33 (s, 6H; $C(O)CH_3$), 2.00 (s, 6H; $ArCH_3$), 1.98 (s, 12H; $ArCH_3$); MALDI-MS: 1003 [M^+], calcd: 1004.3; 1042 [$M\cdot K^+$], calcd: 1043.3.

Synthesis of benzylbromide [6]cavitand 5: [6]Cavitand **1** (1.00 g, 1.12 mmol) and *N*-bromosuccinimide (NBS; 1.27 g, 7.14 mmol) were added to CCl_4 (300 mL), and the mixture was stirred for 30 min at room temperature before a spatula tip of 2,2′-azobis-(2-methylpropionitrile) was added. The flask was irradiated for 15 h (desk lamp, 100 W, ca. 40 cm distance to flask). The solvent was removed under reduced pressure, and chloroform (50 mL) was added. This reaction mixture was purified by column chromatography using chloroform as the eluent. The fractions containing the main product (less polar than [6]cavitand) were combined and precipitated by hexanes to yield [6]cavitand benzyl bromide **5** as a white powder after filtration (0.36 g, 23.5% yield). ^{1}H NMR (500 MHz, $CDCl_3$, $-23\,^\circ$C): $\delta = 7.32$ (s, 2H; ArH; H$_1$), 7.29 (s, 4H; ArH; H$_2$), 6.11 (d, ^2J(H,H) = 7.3 Hz, 2H, OCH_2O; H$_3$), 5.99 (d, ^2J(H,H) = 7.1 Hz, 4H, OCH_2O; H$_4$), 4.70 (d, ^{2}J(H,H) = 7.7 Hz, 4H, OCH_2O; H$_7$), 4.60 (d, ^2J(H,H) = 7.3 Hz, 2H, OCH_2O; H$_6$), 4.57 (d, ^2J(H,H) = 9.0 Hz, 4H, $ArCH_2Br$; H$_{11}$), 4.51 (d, 4H, $ArCH_2Ar$; H$_5$), 4.50 (s, 4H, $ArCH_2Br$; H$_{12}$), 4.41 (d, ^2J(H,H) = 8.9 Hz, 4H, $ArCH_2Br$; H$_{13}$), 4.01 (d, ^2J(H,H) = 13.2 Hz, 2H, $ArCH_2Ar$; H$_8$), 3.34 (d, ^2J(H,H) = 12.3 Hz, 4H, $ArCH_2Ar$; H$_9$), 3.14 (d, ^2J(H,H) = 13.2 Hz, 2H, $ArCH_2Ar$; H$_{10}$). MALDI-MS: 1281 ([M^+], 5Br, 1H); other peaks at about half intensity are at 1199 (4Br, 2H), and 1361 (6Br), calcd. 1361.8.

Synthesis of benzylthiol and benzylthioacetate [6]cavitands 8 and 9

[6]Cavitand benzylthiol 8: A sample of **5** (290 mg, 0.21 mmol) was dissolved in degassed DMF (25 mL). Thiourea was added in excess (220 mg, 2.9 mmol), and the reaction mixture was stirred at ambient temperature under reduced pressure (0.01 mm) for 2 h. A degassed aqueous 2 M NaOH solution (25 mL) was added to the reaction flask, and the reaction mixture was stirred under reduced pressure (ca. 1 mm) for 30 min. The reaction contents were poured into a degassed aqueous acetic acid solution (5 vol%; 200 mL). The mixture was extracted with chloroform three times, and the organic phases were dried and evaporated under reduced pressure. The residue was taken up in chloroform, and subjected to column chromatography using chloroform as the eluent to yield **8** as a white powder after precipitation from hexanes (130 mg, 56% yield). ^{1}H NMR (500 MHz, $CDCl_3$, 27 °C): $\delta = 7.29$ (s, 2H; ArH; H$_1$), 7.22 (s, 4H; ArH; H$_2$), 6.02 (d, ^2J(H,H) = 7.3 Hz, 2H; OCH_2O; H$_3$), 5.95 (d, ^2J(H,H) = 6.9 Hz, 4H; OCH_2O; H$_4$), 4.59 (m, 6H; OCH_2O; H$_{7,6}$), 4.53 (d, ^2J(H,H) = 11.8 Hz, 4H; $ArCH_2Ar$; H$_5$), 3.97 (d, ^{2}J(H,H) = 12.8 Hz, 2H; $ArCH_2Ar$; H$_8$), 3.68–3.59 (m, 12H; $ArCH_2SH$), 3.33 (d, ^2J(H,H) = 12.2 Hz, 4H; $ArCH_2Ar$; H$_9$), 3.14 (d, ^{2}J(H,H) = 12.4 Hz, 2H; $ArCH_2Ar$; H$_{10}$), 1.89 (m, 4H; $ArCH_2SH$), 1.61 (m, 2H; $ArCH_2SH$).

[6]Cavitand benzylthioacetate 9: A small sample of benzylthiol **8** (10 mg) was acetylated by stirring it in pyridine/acetic anhydride solution (5 mL of a 1:1 (v:v) solution) at ambient temperature for 12 h. The solvent was evaporated, and the residue was dissolved in $CHCl_3$ and filtered through a silica gel pad to yield **9** (6 mg; 41% yield). ^{1}H NMR (400 MHz, $CDCl_3$, 26 °C): $\delta = 7.24$ (m, 2H; ArH; H$_1$), 7.20 (s, 4H; ArH; H$_2$), 5.97 (d (br), ^2J(H,H) = 7.3 Hz, 2H; OCH_2O; H$_3$), 5.86 (d, ^2J(H,H) = 7.5 Hz, 4H; OCH_2O; H$_4$), 4.50 (m, 6H; OCH_2O; H$_{7,6}$), 4.28 (m, 8H; $ArCH_2SAc$, $ArCH_2Ar$; H$_{11}$, H$_5$), 4.09 (s, 4H; $ArCH_2SAc$; H$_{12}$), 3.91 (m, 6H; $ArCH_2SAc$, $ArCH_2Ar$; H$_{13}$, H$_8$), 3.30 (m, 4H; $ArCH_2Ar$; H$_9$), 3.09 (m, 2H; $ArCH_2Ar$; H$_{10}$), 2.29 (s, 18H; $C(O)CH_3$); MALDI-MS: 1356 [$M\cdot Na^+$], calcd: 1355.2; 1372 [$\mathbf{M}\cdot K^+$], calcd: 1371.2.

X-ray crystallography: A clear prism-shaped crystal of bisketone **2** (obtained by slow evaporation of [D$_6$]DMSO), with dimensions of $0.40 \times 0.30 \times 0.30$ mm, was mounted on a glass fiber and placed on a Rigaku/ADSC CCD diffractometer under a $-100(1)\,^\circ$C nitrogen stream. Data were collected in 0.50° oscillations with 47.0 s exposures out to a maximum 2θ value of 50.1° using $Mo_{K\alpha}$ radiation ($\lambda = 0.71069$ Å). Data collection was carried out in two scan sets; the first using ω oscillations between -17.0 and 23.0°, the second using ω oscillations between 0.0 and 190.0°. Each scan set was carried out at $\chi = -90.0°$, with the detector swing angle at $-5.59°$ and a crystal-to-detector distance of 38.45 mm. The unit cell was found to be primitive monoclinic, with cell dimensions of $a = 15.9811(6)$, $b = 20.6386(8)$, and $c = 33.842(1)$ Å, $\beta = 96.47(2)°$, and $V = 11090.9(7)$ Å^3. The collected data (71788 reflections in total) were processed and corrected for absorption and Lorentz and polarization effects using the d*TREK program[18] ($\mu = 0.21\,mm^{-1}$, $T_{max} = 0.939$, $T_{min} = 0.920$). The space group was determined to be $P2_1/n$ on the basis of systematic absences. The structure was solved by direct methods[19] and expanded using Fourier techniques.[20] The material crystallizes with two molecules in the asymmetric unit. In addition there are six DMSO solvent molecules in the asymmetric unit. The calculated density is 1.38 gcm^{-3}. Refinements were carried out against $|F^2|$ using SHELXL97.[21] All non-hydrogen atoms were refined anisotropically, while hydrogen atoms were included in calculated positions but were not refined. The final residuals are: $R1 = 0.054$ (12028 reflections with $I > 2\sigma(I)$, 1513 parameters), $wR2 = 0.146$ (using all 19457 reflections, 1513 parameters), with minimum and maximum residual electron density peaks of -0.67 and 0.67 e$^-$ Å^{-3}, respectively.

A clear chip shaped crystal of diol **3** (obtained by slow evaporation of acetone), with dimensions of $0.50 \times 0.50 \times 0.20$ mm, was mounted on a glass fiber and placed on a Rigaku/ADSC CCD diffractometer under a $-100(1)\,^\circ$C nitrogen stream. Data were collected in 0.50° oscillations with 176.0 second exposures out to a maximum 2θ value of 46.5° using Mo$K\alpha$ radiation ($\lambda = 0.71069$ Å). Data collection was carried out in two scan sets; the first using ω oscillations between -17.0 and 23.0°, the second using ϕ oscillations between 0.0 and 190.0°. Each scan set was carried out at $\chi = -90.0°$, with the detector swing angle at $-5.65°$ and a crystal-to-detector distance of 38.14 mm. The unit cell was found to be primitive monoclinic, with cell dimensions of $a = 26.900(3)$, $b = 16.053(1)$, $c = 28.235(2)$ Å, $\beta = 100.98(1)°$, and $V = 11980(2)$ Å^3. The collected data (66042 reflections in total) were processed and corrected for absorption and Lorentz and polarization effects using the d*TREK program[18] ($\mu = 0.09\,mm^{-1}$, $T_{max} = 0.983$, $T_{min} = 0.957$). The space group was determined to be $P2_1/a$ on the basis of systematic absences. The structure was solved by direct methods[19] and expanded using Fourier techniques.[20] The material crystallizes with two molecules in the asymmetric unit. In addition there are six acetone solvent molecules in the asymmetric unit. The calculated density is 1.21 gcm^{-3}. Refinements were carried out against $|F^2|$ using SHELXL97.[21] All non-hydrogen atoms except those of the solvent molecules were refined anisotropically, while hydrogen atoms were included in calculated positions but were not refined. The final residuals are: $R1 = 0.156$ (8579 reflections with $I > 2\sigma(I)$, 1355 parameters), $wR2 = 0.403$ (using all 16872 reflections, 1355 parameters), with minimum and maximum residual electron density peaks of -0.59 and 0.98 e$^-$ Å^{-3}, respectively. The cavitand molecules

© 2002 WILEY-VCH Verlag GmbH & Co. KGaA, Weinheim
0947-6539/02/0816-3722 $ 20.00+.50/0 *Chem. Eur. J.* **2002**, *8*, No. 16

appear to be mildly disordered with respect to the position of their respective hydroxy groups. In the case of both cavitand molecules electron density in geometries consistent with C-O single bonds was found in positions *x′* and *x″*, as described in Figure 3. No significant residual electron density was found in position *y*, which is the conformation found for bisketone **2**. The major and minor disordered OH fragments were refined with anisotropic and isotropic thermal parameters, respectively. Final occupancies were refined to roughly 0.85 and 0.15 for the major and minor fragments. While the final residuals are rather large, this is likely a result of the large quantity of light-atom solvent molecules in the asymmetric unit and the disordered nature of the two cavitand molecules which, taken together, likely diminish the scattering ability of the crystal. CCDC-182302 (**2**) and CCDC-182303 (**3**) contain the supplementary crystallographic data (excluding structure factors) for the structures reported in this paper. These data can be can be obtained free of charge via www.ccdc.cam.ac.uk/conts/retrieving.html (or from the Cambridge Crystallographic Data Centre, 12 Union Road, Cambridge CB2 1EZ, UK; fax: (+44) 1223-336033; or deposit@ccdc.cam.ac.uk).

Acknowledgements

The authors would like to thank NSERC, Canada for financial support.

[1] P. Timmerman, W. Verboom, D. N. Reinhoudt, *Tetrahedron* **1996**, *52*, 2663.
[2] *Calixarenes 2001* (Eds.: Z. Asfari, V. Böhmer, J. Harrowfield, J. Vicens), Kluwer Academic Publishers: Dordrecht, **2001**.
[3] D. J. Cram, J. M. Cram, *Container Molecules and Their Guests*, *Vol. 4*, Royal Society of Chemistry, Cambridge, **1994**.
[4] C. Naumann, E. Román, C. Peinador, T. Ren, B. O. Patrick, A. E. Kaifer, J. C. Sherman, *Chem. Eur. J.* **2001**, *7*, 1637.
[5] C. Naumann, S. Place, J. C. Sherman, *J. Am. Chem. Soc.* **2002**, *124*, 16.
[6] Pulse sequence used: selnogp.2 (Bruker, avance-version (00/02/07): 1D NOESY using selective excitation with a shaped pulse; dipolar coupling may be due to NOE or chemical exchange. K. Stott, J. Stonehouse, J. Keeler, T.-L. Hwang, A. J. Shaka, *J. Am. Chem. Soc.* **1995**,*117*, 4199. See also: C. Naumann, B. O. Patrick, J. C. Sherman, *Tetrahedron* **2002**, *58*, 787.
[7] Longer reaction time did not change the yield, nor the fact that we always isolated as much starting material [6]cavitand **1** as product **2**, even with a large excess of $KMnO_4$.
[8] If the carbonyls were 1,2, there would be at least four different sets of ArH (1:2:2:1) depending on the conformation of the ketones, and none would exchange. If the carbonyls were 1,3, there would be three sets of ArH (2:2:2) but none would interconvert.
[9] For proton labels of bisketone **2**, see Figure 7. For proton labels of diol **3**, see Figure 9.
[10] CS Chem3D Pro was used.
[11] For **3** (and **4**), each of the two hydroxy (acetate) groups can theoretically exist in one of two diastereotopic positions, a or b. In addition, each of these have conformational possibilities **I** (see Figure 9) or **IIa**. The symmetry of the ^{1}H NMR spectra suggests that **3** and **4** are either diastereomer a, a or b, b; diastereomer a, b would have lower symmetry. The large $\Delta\delta$ values for exchanging resonances of **3** and **4** (Table 1) are similar to the values obtained for the prototype [6]cavitand **1** and different from the small values for **2**. Thus, the $\Delta\delta$ of **3** and **4** support conformation **I**. We can assign the structure of **3** (and **4**) to contain both OH (OAc) in "axial" positions (Figure 9) based on the following NOE observations for diol **3** (similar NOEs were observed for bisacetate **4**). NOEs (at $-10\,^\circ$C in [D_6]acetone) between the *para* ArH protons (H_1 and $H_{2''}$) and the hydroxyl OH protons for diol **3** are more than three times larger than those between the *para* ArH (H_1 and $H_{2''}$) and the C*H*(OH) protons. Also, the C*H*(OH) protons have NOEs to the acetal protons $H_{4''}$ and $H_{7''}$, whereas there are no NOEs between the hydroxyl protons and $H_{4''}$ or $H_{7''}$.
[12] MALDI mass spectrometric data of **5** is weak, the molecule fragments readily losing bromines. The main peak is at 1281 (5Br, 1H); other peaks at about half intensity are at 1199 (4Br, 2H), and 1361 (6Br). Better mass spectrometric evidence for benzyl bromide **5** was derived by reacting a few mg of **5** with excess KCN in DMF at ambient temperature overnight. MALDI of the reaction mixture shows two strong peaks: at 1063 (benzyl nitrile **6**·Na^+) and 1079 (**6**·K^+). Second, **5** was reacted with excess NaOAc in DMF (2 h, overnight). The MALDI spectrum shows two strong peaks at 1260 (benzyl acetate **7**·Na^+) and 1276 (**7**·K^+); and the ESI-MS shows a strong peak at 1259 corresponding to **7**·Na^+.
[13] D. J. Cram, S. Karbach, Y. H. Kim, L. Baczynskyj, K. Marti, R. M. Sampson, G. W. Kalleymeyn, *J. Am. Chem. Soc.* **1988**, *110*, 2554.
[14] M. Mutter, P. Dumy, P. Garrouste, C. Lehmann, M. Mathieu, C. Peggion, S. Peluso, A. Razaname, G. Tuchscherer, *Angew. Chem. Int. Ed. Engl.* **1996**, 1482, and references therein.
[15] a) A. R. Mezo, J. C. Sherman, *J. Org. Chem.* **1998**, *63*, 6824; b) A. S. Causton, J. C. Sherman, *Bioorg. Med. Chem.* **1999**, *7*, 23; c) A. R. Mezo, J. C. Sherman, *J. Am. Chem. Soc.* **1999**, 121, 8983.
[16] L. Pirondini, D. Bonifazi, E. Menozzi, E. Wegelius, K. Rissanen, C. Massera, E. Dalcanale, *Eur. J. Org. Chem.* **2001**, 2311.
[17] F. Fochi, P. Jacopozzi, E. Wegelius, K. Rissanen, P. Cozzini, E. Marastoni, E. Fisicaro, P. Manini, R. Fokkens, E. Dalcanale, *J. Am. Chem. Soc.* **2001**, *123*, 7539.
[18] d*TREK: Area Detector Software. Version 7.1I. Molecular Structure Corporation, **2001**.
[19] A. Altomare, M. C. Burla, G. Cammalli, M. Cascarano, C. Giacovazzo, A. Guagliardi, A. G. G. Moliterni, G. Polidori, A. Spagna, *J. Appl. Crystallogr.* **1999**, 32, 115.
[20] P. T. Beurskens, G. Admiraal, G. Beurskens, W. P. Bosman, R. de Gelder, R. Israel, J. M. M. Smits, The DIRDIF-94 program system, Technical Report of the Crystallography Laboratory, **1994**, University of Nijmegen, The Netherlands.
[21] G. M. Sheldrick, **1997**, University of Göttingen, Germany.

Received: December 13, 2001
Revised: April 30, 2002 [F3736]

 © 2002 WILEY-VCH Verlag GmbH & Co. KGaA, Weinheim 0947-6539/02/0816-3723 $ 20.00+.50/0